BOLLETTINO DI GEOFISICA TEORICA ED APPLICATA VOL. 40, N. 3-4, pp. 563-569; SEP.-DEC. 1999

Comparison among different geoid solutions for the Egyptian south-western desert using FFT technique

H. A. ABD-ELMOTAAL

Civil Engineering Department, Faculty of Engineering,
Minia University, Egypt

(Received April 1, 1999; accepted April 6, 1999)

Abstract. Different geoid solutions for the Egyptian south-western desert are carried out in this investigation. The available data for this paper are 2682 measured gravity values and a set of fine 30" × 30" and coarse 3' × 3' Digital Height Models for the area under investigation. The EGM96 geopotential earth model has been used for removing the effect of the reference filed from the gravity data. The geoid is computed using various gravity reduction techniques. They are: the free-air, the Airy-Heiskanen isostatic, the Pratt-Hayford isostatic, the Vening Meinesz isostatic, the Helmert condensation and the Rudzki inversion reduction techniques. The reduced gravity anomalies are gridded on a 3' × 3' geographical grid using the least-squares interpolation technique with local covariance functions. These gridded reduced anomalies are used to compute the different geoid solutions in the frequency domain using the spherical 2D FFT technique. The relative difference between the different geoid solutions has an internal accuracy of about 2.5 cm.

1. Introduction

It is known that, in principle, all gravity reduction techniques should lead to the same geoid if they are properly applied and the indirect effect, if any, is taken into account (Heiskanen and Moritz, 1967, p. 151). The aim of this investigation is to compare different geoid solutions based on various gravity reduction techniques. These techniques involve the free-air, the Airy-Heiskanen isostatic, the Pratt-Hayford isostatic, the Vening Meinesz isostatic, the Helmert condensation and the Rudzki inversion reduction techniques. The geoid is computed in the frequency domain using the spherical 2D FFT technique (Strang van Hees, 1990).

Corresponding author: H. A. Abd-Elmotaal; Minia University, Civil Engineering Department, Faculty of Engineering, Minia 61111, Egypt; phone: +20 86 362083; fax: +20 2 2918059; e-mail: abdelmotaal@mailcity.com

Table 1 - Statistics of the gravity anomalies after removing the EGM96 reference field. All values are in mGal.

reduction type	minimum	maximum	mean	standard deviation
free-air	-21.02	27.33	-1.04	8.35
Airy-Heiskanen isostatic	-28.14	25.17	-5.90	8.41
Pratt-Hayford isostatic	-31.27	23.08	-8.81	8.52
Vening Meinesz isostatic	-28.32	25.32	-5.51	8.38
Helmert condensation	-21.00	28.26	-1.39	8.49
Rudzki inversion	-20.77	28.68	-0.92	8.74

2. The data

A set of 2682 measured gravity stations is available for this investigation. These stations are located in the data window ($22° \le \phi \le 25°$, $27.5° \le \lambda \le 30°$). The values of the measured gravity are ranging between 978 665.6 mGals and 978 889.1 mGals with an average of 978 757.1 mGals and a standard deviation of about 47 mGals. For the terrain reduction computation, a set of fine and coarse Digital Height Models (DHM's) is needed. A 30" × 30" fine DHM for the data window is available. The heights range between 148 m and 563 m with an average of 312 m and a standard deviation of about 71 m. A 3' × 3' coarse DHM is available for a larger window ($20.5° \le \phi \le 26.5°$, $26 \le \lambda \le 31.5°$). Both models are extracted from the global 30" × 30" DHM provided by the NOAA.

3. Gravity reduction techniques

The gravity reduction techniques used in this investigation involve the freeair, the Airy-Heiskanen isostatic, the Pratt-Hayford isostatic, the Vening Meinesz isostatic, the Helmert condensation and the Rudzki inversion reduction techniques. For more details concerning the theoretical background of these techniques, the reader is kindly asked to refer to (Heiskanen and Moritz, 1967). For the Vening Meinesz isostatic model, the reader is invited to refer to (Abd-Elmotaal, 1993). The necessary formulas for the Helmert condensation reduction may be found in (Heck, 1993).

The TC-program originally written by Forsberg (1984) has been used in the gravity reduction process after a great modification made by Abd-Elmotaal (1998). For the recovery of the long wavelength part of the gravity field, the EGM96 has been used for the remove-restore process. Table 1 lists the statistics of the gravity anomalies after removing the effect of the EGM96 reference field.

The reduced gravity anomalies are gridded on a 3' × 3' geographical grid using the least-squares interpolation technique with local covariance functions. For more details about that gridding technique and the used covariance function models, the reader is kindly invited to see, for example, (Abd-Elmotaal, 1992; Kraiger, 1988).

4. Stokes' integral using spherical 2D FFT technique

The geoid undulation N can be computed from the gridded gravity anomalies Δg by using the well-known Stokes' integral (Heiskanen and Moritz, 1967, p. 94)

$$N = \frac{R}{4\pi\gamma} \iint_{\sigma} \Delta g \;\; S(\psi) d\sigma, \tag{1}$$

where γ is the normal gravity, R is the mean earth's radius and $S(\psi)$ stands for the Stokes' function given by Heiskanen and Moritz (1967, p. 94)

$$S(\psi) = \frac{1}{S} - 4 - 6s + 10s^2 - \left(3 - 6s^2\right)\ln\left(s + s^2\right) \tag{2}$$

with

$$s = \sin\frac{\psi}{2}, \tag{3}$$

and ψ is the spherical distance between the computational point P and the running point Q, given by Strang van Hees (1990, p. 236)

$$\sin^2\frac{1}{2}\psi_{PQ} = \sin^2\frac{1}{2}(\phi_P - \phi_Q) + \sin^2\frac{1}{2}(\lambda_P - \lambda_Q)\cos\phi_P\cos\phi_Q. \tag{4}$$

For discrete integration the area is divided into blocks of equal $\Delta\phi$ and $\Delta\lambda$, so that the Stokes' integral (1) can be replaced by the summation

$$N(\phi_P, \lambda_P) = \frac{R\Delta\phi\Delta\lambda}{4\pi\gamma} \sum_{Q} (\Delta g_Q \cos\phi_Q) S(\psi_{PQ}). \tag{5}$$

When P coincides with Q, this leads to a singularity problem. In this case, the central block has to be excluded and computed separately. If the central area were a circle of radius r, the contribution N_i to the geoid undulation is given by (Heiskanen and Moritz, 1967, p. 122)

$$N_i = \frac{r}{\gamma}\Delta g. \tag{6}$$

Only a small error will happen if we use (6) for a rectangular block. In this case, r is computed in such a way that the circle would have the same area as the rectangular block, i.e.,

$$r = R\sqrt{\frac{\Delta\phi\Delta\lambda\cos\phi}{\pi}}. \tag{7}$$

The Stokes' integral (1) would be a convolution integral if the spherical distance ψ_{PQ} were a

function of (ϕ_P - ϕ_Q) and (λ_P - λ_Q) only. Eq. (4) shows that ψ_{PQ} is a function of (ϕ_P - ϕ_Q) and (λ_P - λ_Q) as well as of ϕ_P and ϕ_Q . Consequently, Eq. (1) does not fulfill the requirement of a convolution integral. However, if we replace ϕ_P and ϕ_Q by the mean latitude of the area ϕ_m , Eq. (4) will then be given by

$$\sin^2 \frac{1}{2}\psi_{PQ} = \sin^2 \frac{1}{2}(\phi_P - \phi_Q) + \sin^2 \frac{1}{2}(\lambda_P - \lambda_Q)\cos^2 \phi_m, \tag{8}$$

which is a function of (ϕ_P - ϕ_Q) and ($\lambda_P - \lambda_Q$) only. Note that ϕ_m is a constant for the whole area. Thus (1) is now a full convolution integral. Eq. (1) can symbolically be written in a convolution integral form as

$$N(\phi_P, \lambda_P) = \frac{R\Delta\phi\Delta\lambda}{4\pi\gamma}\left[\Delta g_Q \cos\phi_Q * S(\psi_{PQ})\right]. \tag{9}$$

By using the FFT technique, Eq. (9) can be written as (Schwarz et al., 1990)

$$N(\phi_P, \lambda_P) = \frac{R\Delta\phi\Delta\lambda}{4\pi\gamma} F^{-1}\left\{F\left(\Delta g_Q \cos\phi_Q\right)F\left[S(\psi_{PQ})\right]\right\}, \tag{10}$$

where F and F^{-1} stand for the Fourier transform and the inverse Fourier transform, respectively. Eq. (10) is the simple spherical 2-D FFT approach given by Strang van Hees (1990).

5. Geoid solutions and comparisons

The geoids computed from the different gravity reduction techniques are shown in Figs. 1 to 3. The statistics of these geoids are listed in Table 2. Comparing the different geoid solutions immediately shows that the structure of the geoid in the eastern part of the result window is nearly the same. Some differences are remarkable in the western part. In general, all isostatic geoids have nearly the same structure. The free-air and the Rudzki inversion geoids have the same features. They are slightly different from the Helmert condensation geoid.

Fig. 4a shows the absolute difference between the Vening Meinesz (representing the isostatic

Table 2 - Statistics of the different geoid solutions. All values are in meters.

reduction type	minimum	maximum	mean	standard deviation
free-air	12.23	13.92	13.43	0.36
Airy-Heiskanen isostatic	12.24	14.14	13.48	0.42
Pratt-Hayford isostatic	12.19	14.22	13.46	0.45
Vening Meinesz isostatic	12.30	14.24	13.55	0.43
Helmert condensation	12.21	13.88	13.36	0.36
Rudzki inversion	12.30	13.95	13.43	0.37

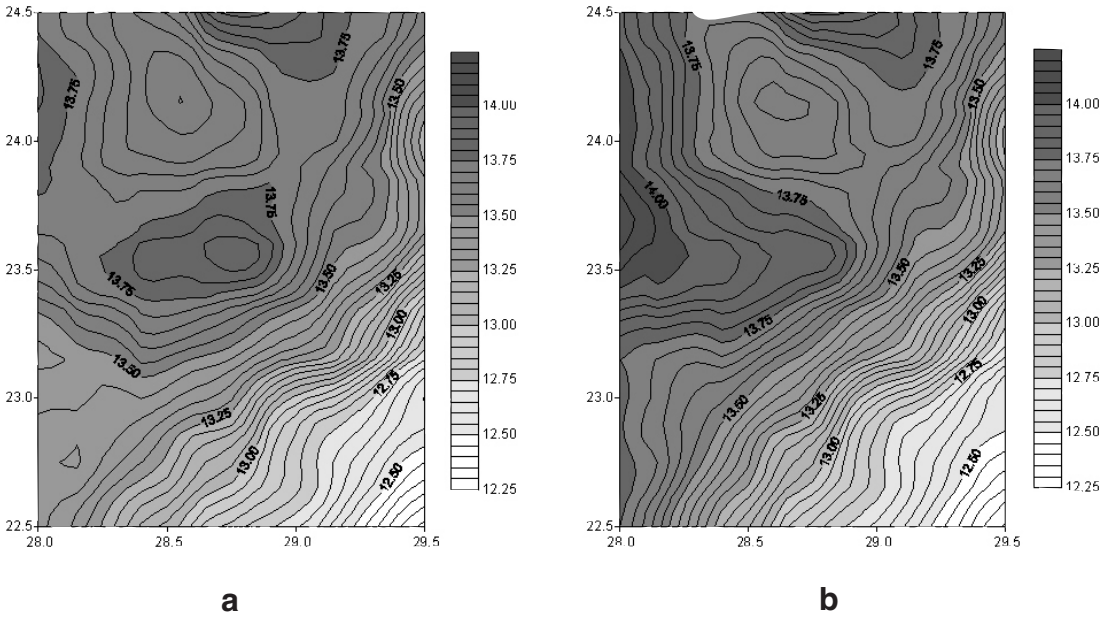

Fig. 1 - (a) The free-air geoid. (b) The Airy-Heiskanen isostatic geoid. Contour interval: 5 cm.

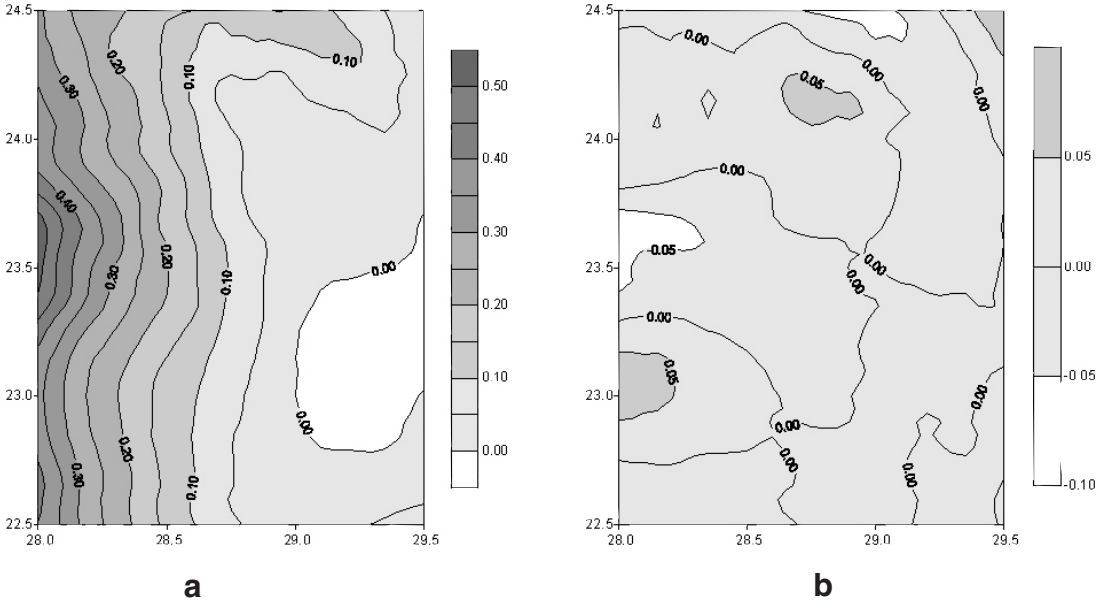

Fig. 2 - (a) The Pratt-Hayford isostatic geoid. (b) The Vening Meinesz isostatic geoid. Contour interval: 5 cm.

geoid) and the free-air geoids. These differences range between –0.05 m and 0.53 m with an average of –0.13 m and a standard deviation of about 0.13 m. Fig. 4a shows some trend behaviour for these differences. This trend has been removed using a third degree surface

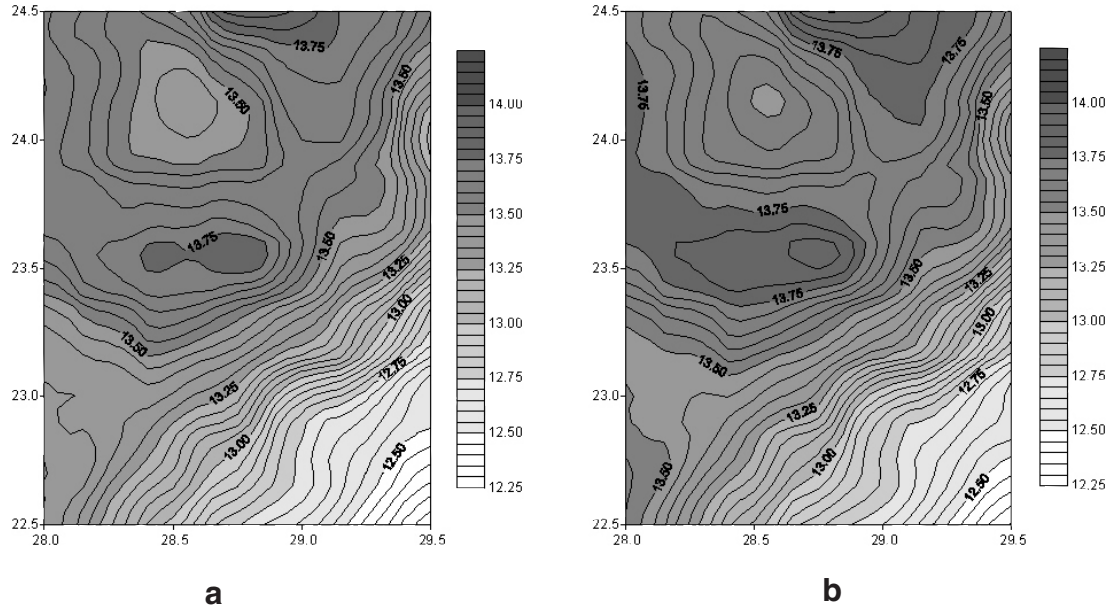

Fig. 3 - (a) The Helmert condensation geoid. (b) The Rudzki inversion geoid. Contour interval: 5 cm.

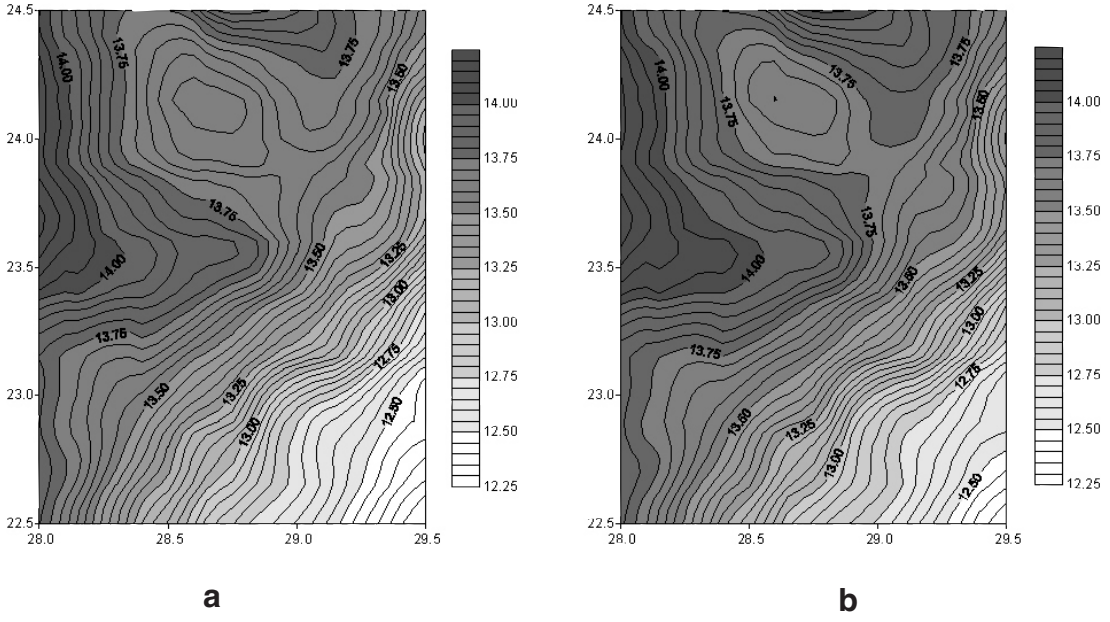

Fig. 4 - (a) Absolute difference between the Vening Meinesz isostatic and the free-air geoids. (b) Difference between the Vening Meinesz isostatic and the free-air geoids after removing a third degree trend surface polynomial. Contour interval: 5 cm.

polynomial. Fig. 4b shows the difference between the Vening Meinesz isostatic and the free-air geoids after removing the trend. These differences range between -8 cm and 8 cm with a standard deviation of about 2.5 cm.

6. Conclusions

The geoid has been computed for the Egyptian south-western desert using free-air, Airy-Heiskanen isostatic, Pratt-Hayford isostatic, Vening Meinesz isostatic, Helmert condensation and Rudzki inversion gravity reduction techniques in the frequency domain using the spherical 2D FFT technique. The isostatic geoids have nearly the same structure. The free-air and the Rudzki inversion geoids have the same feature. The relative difference between the free-air and the Vening Meinesz isostatic geoids has an internal accuracy of about 2.5 cm.

References

Abd-Elmotaal H.; 1992: *Statistical Behaviour of the Free-air, Bouguer and Isostatic Anomalies in Austria.* Bulletin Géodésique, **67**, 86-90.

Abd-Elmotaal H.; 1993: *Vening Meinesz Moho Depths: Traditional, Exact and Approximated.* Manuscripta Geodaetica, **18**, 171-181.

Abd-Elmotaal H.; 1998: *Gravity Reduction Techniques and their Comparisons Applied to the Gravity Field in Egypt.* In: M. Vermeer and J. Ádám (eds), Second Continental Workshop on the Geoid in Europe, Reports of the Finnish Geodetic Institute, **98:4**, pp. 177-183.

Forsberg R.; 1984: *A Study of Terrain Reductions, Density Anomalies and Geophysical Inversion Methods in Gravity Field Modelling.* Reports of the Department of Geodetic Science, **355**, The Ohio State University, Columbus, Ohio, 129 pp.

Heck B; 1993: *A Revision of Helmert's Second Method of Condensation in Geoid and Quasigeoid Determination.* In: H. Montag and Reigber C. (eds), Geodesy and Physics of the Earth. International Association of Geodesy Symposia, **112**, Springer, Berlin, Heidelberg, New York, pp. 246-251.

Heiskanen W. A. and Moritz H.; 1967: *Physical Geodesy.* Freeman, San Francisco, 364 pp.

Kraiger G.; 1988: *Influence of the Curvature Parameter on Least-Squares Prediction*. Manuscripta Geodaetica, **13**, 164-171.

Strang van Hees G.; 1990: *Stokes Formula Using Fast Fourier Techniques.* Manuscripta Geodaetica, **15**, 235-239.

Schwarz K. P., Sideris M. G. and Forsberg R.; 1990: *The Use of FFT Technique in Physical Geodesy.* Geophys. J. Int., **100**, 485-514.